Least-Squares Padé approximation of parametric and stochastic Helmholtz maps

Francesca Bonizzoni[♯,*], Fabio Nobile[§], Ilaria Perugia[♯,†], Davide Pradovera[§]

[♯] Faculty of Mathematics, University of Vienna
Oskar-Morgenstern-Platz 1,1090 Wien, Austria
francesca.bonizzoni@univie.ac.at, ilaria.perugia@univie.ac.at

[§] CSQI – MATH, Ecole Polytechnique Fédérale de Lausanne
Station 8, CH-1015 Lausanne, Switzerland
fabio.nobile@epfl.ch, davide.pradovera@epfl.ch

Abstract

The present work deals with the rational model order reduction method based on the single-point Least-Square (LS) Padé approximation technique introduced in [3]. Algorithmical aspects concerning the construction of the rational LS-Padé approximant are described. In particular, the computation of the Padé denominator is reduced to the calculation of the eigenvector corresponding to the minimal eigenvalue of a Gramian matrix. The LS-Padé technique is employed to approximate the frequency response map associated with various parametric time-harmonic acoustic wave problems, namely, a transmission/reflection problem, a scattering problem, and a problem in high-frequency regime. In all cases we establish the meromorphy of the frequency response map. The Helmholtz equation with stochastic wavenumber is also considered. In particular, for Lipschitz functionals of the solution and their corresponding probability measures, we establish weak convergence of the measure derived from the LS-Padé approximant to the true one. 2D numerical tests are performed, which confirm the effectiveness of the approximation method.

Keywords: Hilbert space-valued meromorphic maps, Padé approximants, convergence of Padé approximants, parametric Helmholtz equation, PDE with random coefficients.

AMS Subject Classification: 30D30, 41A21, 41A25, 35A17, 35J05, 35R60, 65D15

1 Introduction

Many applications require the fast and accurate numerical evaluation of Helmholtz frequency response functions, i.e., functions that map the wavenumber to the solution (or some quantity of interest related to the solution) of the corresponding time-harmonic wave-problem, for a large number of frequencies. In mid- and high-frequency regimes,

very fine meshes or high polynomial degrees should be considered, in order to obtain accurate Finite Element (FE) solutions of the time-harmonic wave-problem. Moreover, low order FE schemes are affected by the pollution effect [2], namely, an increasing discrepancy between the best approximation error and the FE error, as the wave number increases. In the "many-queries" context, i.e., when many solutions of the underlying Partial Differential Equation (PDE) are needed, the "brute force" approach entails the solution of a large number of high-dimensional linear systems, and it is then out of reach.

Model order reduction methods aim at significantly reducing the computational cost by approximating the quantity of interest starting from evaluations at only few wavenumbers. They rely on a two-step strategy: the OFFLINE stage consists in the computation of a finite dimensional basis - e.g., the basis of snapshots (see, e.g., [5, 14, 19, 25, 26, 28, 29, 15, 8, 22]), or evaluations of the frequency response map and its derivatives at fixed centers (Padé method, see, e.g., [7, 13, 10, 9, 3]); the output of this phase, whose computational cost may be very high, is stored, to be used during the ONLINE phase, in which the approximation of the frequency response map corresponding to a given new value of the parameter is constructed. This stage does not involve the numerical solution of any PDE, and is expected to provide the output in real time.

In this work, we focus on the Padé-based model order reduction technique introduced in [3], defined for any given univariate Hilbert space-valued meromorphic map $\mathcal{T} : \mathbb{C} \to V$, and relying on a *single-point Least-Square (LS) Padé approximant*. In particular, the single-point LS-Padé approximant of $\mathcal{T}$ centered in $z_0 \in \mathbb{C}$, denoted by $\mathcal{T}_{[M/N]}$, is given by the rational V-valued map $\mathcal{T}_{[M/N]}(z) = \frac{\mathcal{P}_{[M/N]}(z)}{\mathcal{Q}_{[M/N]}(z)}$, where $\mathcal{P}_{[M/N]}(z) = \sum_{\alpha=0}^{M} p_\alpha (z - z_0)^\alpha$, with coefficients $p_\alpha \in V$ (we write $\mathcal{P}_{[M/N]} \in \mathbb{P}_M(\mathbb{C}; V)$), and $\mathcal{Q}_{[M/N]} \in \mathbb{P}_N^\star(\mathbb{C})$, where $\mathbb{P}_N^\star(\mathbb{C})$ is the set of all polynomials with complex coefficients $\{q_\alpha\}_{\alpha=0}^{N}$ such that $\sum_{\alpha=0}^{N} |q_\alpha|^2 = 1$.

In [3] we have analyzed the convergence of $\mathcal{T}_{[M/N]}$ to $\mathcal{T}$ as $M \to \infty$ for a fixed denominator degree N. In particular, the LS-Padé approximant $\mathcal{T}_{[M/N]}$ identifies the N poles of $\mathcal{T}$ closest to the center z_0, as limit of the roots of the denominator $\mathcal{Q}_{[M/N]}(z)$ for M going to $+\infty$.

In this paper, we describe in detail the *algorithmical aspects* of the construction of the single-point LS-Padé approximant. In particular, the identification of the LS-Padé denominator is proved to be equivalent to the identification of the normalized eigenvector corresponding to the smallest non-negative eigenvalue of the Gramian matrix of the set $\left\{ \mathcal{T}(z_0), (\mathcal{T})_{1,z_0}, \dots, (\mathcal{T})_{N,z_0} \right\}$, where $(\mathcal{T})_{\alpha,z_0}$ denotes the Taylor coefficient of $\mathcal{T}$ of order α at z_0.

Moreover, we explore the effectiveness of the single-point LS-Padé technique when applied to *parametric* frequency response problems which go beyond the setting considered in [3], namely, a *transmission/reflection* problem, and a *scattering* problem. In both cases, we first prove that the frequency response map associated with the considered problem is meromorphic. 2D numerical results are provided, which demonstrate the convergence of the LS-Padé approximation. Moreover, 2D numerical tests in *high-frequency* regime are performed for the parametric problem presented in [3].

The *stochastic* Helmholtz boundary value problem is also considered. We refer to [23] for Uncertainty Quantification for frequency responses in vibroacoustics, to [6, 17, 16] for model order reduction for random frequency responses in structural dynamics, and to [24, 12] for the stochastic Helmholtz equation with uncertainty arising either in the forcing term or in the boundary data or in the shape of the scatterer.

Within the present framework, we propose a novel approach to the *stochastic* Helm-

holtz boundary value problem based on the LS-Padé technique, where the wavenumber k^2 is modeled as a random variable taking values into $K = [k_{min}^2, k_{max}^2]$. We approximate the random variable $X := \mathcal{L}(\mathcal{S}(k^2))$ with $X_P := \mathcal{L}(\mathcal{S}_{[M/N]}(k^2))$. Here, $\mathcal{L} : V \to \mathbb{R}$ is a Lipschitz functional representing a quantity of interest, $\mathcal{S}$ is the meromorphic frequency response map associated with the (stochastic) Helmholtz equation endowed with either homogeneous Dirichlet or homogeneous Neumann boundary conditions, and $\mathcal{S}_{[M/N]}$ is the LS-Padé approximation of $\mathcal{S}$. An upper bound on the approximation error for the characteristic function is derived.

All the considered boundary value problems fall into the following general setting. Let D be an open connected bounded Lipschitz domain in $\mathbb{R}^d$ ($d = 1, 2, 3$), and consider the following Helmholtz boundary value problem

$$\begin{cases} -\Delta u - k^2 \varepsilon_r \ u = f & \text{in } D, \\ u = g_D & \text{on } \Gamma_D, \\ \nabla u \cdot \mathbf{n} = g_N & \text{on } \Gamma_N, \\ \nabla u \cdot \mathbf{n} - iku = g_R & \text{on } \Gamma_R, \end{cases} \qquad (1)$$

where the wavenumber k^2 is either a parameter or a random variable, which takes values into an interval of interest $K := [k_{min}^2, k_{max}^2] \subset \mathbb{R}^+$, $\varepsilon_r = \varepsilon_r(\mathbf{x}) \in L^\infty(D)$, $f \in L^2(D)$, $g_D \in H^{1/2}(\Gamma_D)$, $g_N \in H^{-1/2}(\Gamma_N)$, $g_R \in H^{-1/2}(\Gamma_R)$, and $\{\Gamma_D, \Gamma_N, \Gamma_R\}$ is a partition of ∂D, i.e., $\overline{\Gamma}_D \cup \overline{\Gamma}_N \cup \overline{\Gamma}_R = \partial D$ and $\Gamma_D \cap \Gamma_N = \Gamma_D \cap \Gamma_R = \Gamma_N \cap \Gamma_R = \emptyset$. Throughout the paper, we denote with V the Hilbert space $H^1_{\Gamma_D}(D)$. Moreover we assume the functions in V to be complex-valued.

The outline of the paper is the following. In Section 2, we recall the definition of the single-point LS-Padé approximant and the main convergence result of [3]. In Section 3, we describe the algorithm to compute the LS-Padé approximant. Section 4 deals with a parametric transmission/reflection problem, whereas Section 5 deals with a parametric scattering problem. In Section 6, the LS-Padé approximation is tested in high-frequency regime, and in Section 7 the LS-Padé methodology is applied to the stochastic setting. Finally, conclusions are drawn in Section 8.

2 Least-Squares Padé approximant of the parametric model problem

This section deals with the Least-Squares (LS) Padé approximation of the following parametric Helmholtz problem:

Problem 1 (Parametric Model Problem) *The Helmholtz equation* (1) *has parametric wavenumber* $k^2 \in K := [k_{min}^2, k_{max}^2] \subset \mathbb{R}^+$, $\varepsilon_r = 1$, *and is endowed with either Dirichlet or Neumann homogeneous boundary conditions on* ∂D, *i.e.,* $\Gamma_R = \emptyset$ *and either* $\Gamma_D = \partial D$ *and* $g_D = 0$, *or* $\Gamma_N = \partial D$ *and* $g_N = 0$.

The following result was proved in [3].

Theorem 2.1 *Let* $\mathcal{S}$ *be the frequency response map which associates to each* $z \in \mathbb{C}$, *the solution* $u_z \in V$ *of the weak formulation of Problem 1:*

$$\int_D \nabla u_z(\mathbf{x}) \cdot \overline{\nabla v}(\mathbf{x}) \ d\mathbf{x} - z \int_D u_z(\mathbf{x}) \overline{v}(\mathbf{x}) \ d\mathbf{x} = \int_D f(\mathbf{x}) \overline{v}(\mathbf{x}) \ d\mathbf{x} \quad \forall v \in V. \qquad (2)$$

Then, $\mathcal{S}$ is well-defined, i.e., problem (2) admits a unique solution for any $z \in \mathbb{C} \setminus \Lambda$, Λ being the set of (real, non negative) eigenvalues of the Laplace operator with the

3

considered boundary conditions. Moreover, $\mathcal{S}$ is meromorphic in $\mathbb{C}$, with a pole of order one in each $\lambda \in \Lambda$.

Remark 2.2 *For the sake of simplicity, in Problem 1 we endow the Helmholtz equation with either homogeneous Dirichlet or homogeneous Neumann boundary conditions. Small modifications to the proofs of Theorem 3.1, Proposition 4.1, and Proposition 4.2 in [3] allow to handle both homogeneous mixed Dirichlet/Neumann and non-homogeneous Neumann boundary conditions, and to conclude an analogous result as Theorem 2.1. In Section 4, we will show how to handle non-homogeneous Dirichlet boundary conditions.*

We recall now the definition and the convergence theorem of the LS-Padé approximant of the frequency response map $\mathcal{S}$.

Let $K = [k_{min}^2, k_{max}^2] \subset \mathbb{R}^+$ be the interval of interest, and $z_0 \in \mathbb{C} \setminus \Lambda$ with $\mathrm{Re}(z_0) > 0$. To fix the ideas we take $z_0 = \frac{k_{min}^2 + k_{max}^2}{2} + \delta i$, with $\delta \in \mathbb{R} \setminus \{0\}$ arbitrary. The LS-Padé approximant of $\mathcal{S}$, centered in z_0, is given by the ratio of two polynomials of degree M and N respectively:

$$\mathcal{S}_{[M/N]}(z) := \frac{\mathcal{P}_{[M/N]}(z)}{\mathcal{Q}_{[M/N]}(z)}. \tag{3}$$

The denominator $\mathcal{Q}_{[M/N]}(z)$ is a function of z only, and belongs to the space $\mathbb{P}_N^\star(\mathbb{C})$ of all polynomials of degree at most N, $q = \sum_{i=0}^N q_i (z - z_0)^i \in \mathbb{P}_N(\mathbb{C})$, such that $\sum_{i=0}^N |q_i|^2 = 1$. The numerator $\mathcal{P}_{[M/N]} : \mathbb{C} \to V$ is a function of both the complex variable z and the space variable $\mathbf{x} \in D$. More precisely, $\mathcal{P}_{[M/N]}(z) = \sum_{i=0}^M p_i (z - z_0)^i$, with coefficients $p_i \in V$. In the following, we denote with $\mathbb{P}_M(\mathbb{C}; V)$ the space of polynomials of degree at most M in $z \in \mathbb{C}$ with coefficients in V.

The construction of the LS-Padé approximant proposed in [3] relies on the minimization of the functional $j_{E,\rho} : \mathbb{P}_M(\mathbb{C}; V) \times \mathbb{P}_N^\star(\mathbb{C}) \to \mathbb{R}$, parametric in $E \in \mathbb{N}$ and $\rho \in \mathbb{R}^+$, defined as

$$j_{E,\rho}(P, Q) = \left(\sum_{\alpha=0}^E \left\| \left(Q(z)\mathcal{S}(z) - P(z) \right)_{\alpha, z_0} \right\|_{V, \sqrt{\mathrm{Re}(z_0)}}^2 \rho^{2\alpha} \right)^{1/2}, \tag{4}$$

where the brackets $(\cdot)_{\alpha, z_0}$ denote the α-th Taylor coefficient of the Taylor series centered in z_0 (i.e., for a map $\mathcal{T} : \mathbb{C} \setminus \Lambda \to V$, $\left(\mathcal{T}(z) \right)_{\alpha, z_0} = \frac{1}{\alpha!} \frac{d^\alpha \mathcal{T}}{dz^\alpha}(z_0)$), and $\|\cdot\|_{V, \sqrt{\mathrm{Re}(z_0)}}$ denotes the weighted $H^1(D)$-norm (equivalent to the standard one) defined as

$$\|v\|_{V, \sqrt{\mathrm{Re}(z_0)}} := \sqrt{\|\nabla v\|_{L^2(D)}^2 + \mathrm{Re}(z_0) \|v\|_{L^2(D)}^2}. \tag{5}$$

We recall the formal definition of the LS-Padé approximant of the solution map $\mathcal{S}$, and we refer to Section 3 for the proof of the existence of a (not in general unique) LS-Padé approximant.

Definition 2.3 *Let $M, N \in \mathbb{N}$, $E \geq M + N$, and $\rho \in \mathbb{R}^+$. A LS-Padé approximant $\mathcal{S}_{[M/N]}$, centered in z_0, of the solution map $\mathcal{S}$ is a quotient $\frac{P}{Q}$ with $P \in \mathbb{P}_M(\mathbb{C}; V)$, $Q \in \mathbb{P}_N^\star(\mathbb{C})$, such that*

$$j_{E,\rho}(P, Q) \leq j_{E,\rho}(R, S) \quad \forall R \in \mathbb{P}_M(\mathbb{C}; V), \ \forall S \in \mathbb{P}_N^\star(\mathbb{C}). \tag{6}$$

The following convergence result has been proved in [3].

Theorem 2.4 *Let $N \in \mathbb{N}$ be fixed, and let $R \in \mathbb{R}^+$ be such that the disk $\overline{\mathcal{B}(z_0, R)}$ contains exactly N poles of $\mathcal{S}$. Then, for any $z \in \mathcal{B}(z_0, R) \setminus \Lambda$ and for any $|z| < \rho < R$, it holds*

$$\lim_{M \to \infty} \left\| \mathcal{S}(z) - \mathcal{S}_{[M/N]}(z) \right\|_{V, \sqrt{\mathrm{Re}(z_0)}} = 0,$$

for all $E \geq M + N$. Moreover, given $\alpha > 0$ small enough, introduce the open subset

$$K_\alpha := \bigcup_{\lambda \in \Lambda \cap K} (\lambda - \alpha, \lambda + \alpha) \subset K.$$

Then for any $0 < \rho < R$ such that $\mathcal{B}(z_0, \rho) \supset K$, there exists $M^\star \in \mathbb{N}$ such that, for any $M \geq M^\star$ and for any $z \in K \setminus K_\alpha$, it holds

$$\left\| \mathcal{S}(z) - \mathcal{S}(z)_{[M/N]} \right\|_{V, \sqrt{\mathrm{Re}(z_0)}} \leq C \frac{1}{\alpha^3} \left(\frac{\rho}{R} \right)^{M+1}, \tag{7}$$

where the constant $C > 0$ depends on ρ, R, N, z_0, $\lambda_{min} = \min\{\lambda \in \Lambda\}$, $\|f\|_{L^2(D)}$, and $g(z) = \prod_{\lambda \in \Lambda \cap \mathcal{B}(z_0, R)} (z - \lambda)$.

Remark 2.5 *In [3] the bound*

$$\left\| \mathcal{S}(z) - \mathcal{S}(z)_{[M/N]} \right\|_{V, \sqrt{\mathrm{Re}(z_0)}} \leq C \frac{1}{\alpha} \left(\frac{\rho}{R} \right)^{M+1}$$

was proved, with a constant C that depends on $\frac{1}{g_{K \setminus K_\alpha}^2}$, with

$$g_{K \setminus K_\alpha} := \min_{z \in K \setminus K_\alpha} |g(z)|,$$

and $g(z) = \prod_{\lambda \in \Lambda \cap \mathcal{B}(z_0, R)} (z - \lambda)$. Since the frequency response map $\mathcal{S}$ presents only simple poles (given by the Dirichlet/Neumann Laplace eigenvalues), and the interval of interest K contains a finite number of poles of $\mathcal{S}$, it follows that there exists $C_g > 0$ such that

$$|g(z)| \geq C_g \min_{\lambda \in \Lambda \cap \mathcal{B}(z_0, R)} |z - \lambda| \quad \forall z \in K,$$

hence $g_{K \setminus K_\alpha} \geq C_g \alpha$ and the bound (7) follows.

We can draw the following consequences:

(a) The roots of the LS-Padé denominator $\mathcal{Q}_{[M/N]}$ approximate the N poles of $\mathcal{S}$, closest to z_0.

(b) The region of convergence of $\mathcal{S}_{[M/N]}$ is an open circle whose radius is equal to the distance between z_0 and the $(N + 1)$-th closest pole of $\mathcal{S}$.

3   Algorithmical aspects

In this section, we describe an algorithm for the computation of a LS-Padé approximant (defined according to Definition 2.3) of the Helmholtz frequency response map $\mathcal{S}$ introduced in the previous section. We underline that the presented algorithm can be likewise applied to any V-valued meromorphic map $\mathcal{T} : \mathbb{C} \to V$. As a first instructive step, we recall the proof of the existence of such an approximant, which was developed in [3, Proposition 4.1].

Proposition 3.1 *For any $M, N \in \mathbb{N}$, $E \geq M + N$, and $\rho \in \mathbb{R}^{+}$, there exists a LS-Padé approximant centered in z_0.*

Proof. We want to show that the minimization problem (6) admits at least one solution. Since P has degree M, then $\big(P(z)\big)_{\alpha, z_0} = 0$ for all $\alpha > M$. Hence, we can rewrite $j_{E, \rho}$ as

$$
\begin{aligned}
j_{E, \rho}(P, Q)^2 &= \sum_{\alpha=0}^{M} \left\| \big(Q(z)\mathcal{S}(z) - P(z)\big)_{\alpha, z_0} \right\|_{V, \sqrt{\mathrm{Re}(z_0)}}^2 \rho^{2\alpha} \\
&\quad + \sum_{\alpha=M+1}^{E} \left\| \big(Q(z)\mathcal{S}(z) - P(z)\big)_{\alpha, z_0} \right\|_{V, \sqrt{\mathrm{Re}(z_0)}}^2 \rho^{2\alpha} \\
&= \sum_{\alpha=0}^{M} \left\| \big(Q(z)\mathcal{S}(z) - P(z)\big)_{\alpha, z_0} \right\|_{V, \sqrt{\mathrm{Re}(z_0)}}^2 \rho^{2\alpha} \\
&\quad + \sum_{\alpha=M+1}^{E} \left\| \big(Q(z)\mathcal{S}(z)\big)_{\alpha, z_0} \right\|_{V, \sqrt{\mathrm{Re}(z_0)}}^2 \rho^{2\alpha}.
\end{aligned}
$$

Now, let Q be fixed. Taking $P = \bar{P}(Q)$, where $\bar{P}(Q)$ satisfies

$$
\big(\bar{P}(z)\big)_{\alpha, z_0} = \big(Q(z)\mathcal{S}(z)\big)_{\alpha, z_0} \quad \forall\, 0 \leq \alpha \leq M,
$$

problem (6) can be formulated as a minimization problem in Q only: find $Q \in \mathbb{P}_N^{\star}(\mathbb{C})$ such that

$$
\bar{j}_{E, \rho}(Q) \leq \bar{j}_{E, \rho}(S) \quad \forall S \in \mathbb{P}_N^{\star}(\mathbb{C}), \tag{8}
$$

where

$$
\bar{j}_{E, \rho}(Q) := j_{E, \rho}(\bar{P}(Q), Q) = \left(\sum_{\alpha=M+1}^{E} \left\| \big(Q(z)\mathcal{S}(z)\big)_{\alpha, z_0} \right\|_{V, \sqrt{\mathrm{Re}(z_0)}}^2 \rho^{2\alpha} \right)^{1/2}. \tag{9}
$$

Since the functional $\bar{j}_{E, \rho}$ is continuous and the set $\mathbb{P}_N^{\star}(\mathbb{C})$ is compact (being homeomorphic to the unit sphere in $\mathbb{C}^{N+1}$), $\bar{j}_{E, \rho}$ has a global minimum on $\mathbb{P}_N^{\star}(\mathbb{C})$, and the minimization problem (8) admits at least one solution. $\qquad\square$

In the following proposition we express an equivalent formulation of the constrained minimization problem (8).

Proposition 3.2 *The constrained minimization problem (8) is equivalent to the identification of the (normalized) eigenvector corresponding to the smallest non-negative eigenvalue of the Hermitian positive-semidefinite matrix $G_{E, \rho} \in \mathbb{C}^{(N+1) \times (N+1)}$ with entries*

$$
(G_{E, \rho})_{i, j} = \sum_{\alpha=M+1}^{E} \left\langle \big(\mathcal{S}\big)_{\alpha-j, z_0}, \big(\mathcal{S}\big)_{\alpha-i, z_0} \right\rangle_{V, \sqrt{\mathrm{Re}(z_0)}} \rho^{2\alpha}, \qquad i, j = 0, \ldots, N, \tag{10}
$$

where $\langle \cdot, \cdot \rangle_{V, \sqrt{\mathrm{Re}(z_0)}}$ denotes the scalar product that induces the weighted $H^1(D)$-norm $\|\cdot\|_{V, \sqrt{\mathrm{Re}(z_0)}}$, and the Taylor coefficient of order β, $\big(\mathcal{S}\big)_{\beta, z_0}$, is the unique solution of the following Helmholtz equation:

$$
\begin{aligned}
\int_D \nabla\big(\mathcal{S}\big)_{\beta, z_0}(\mathbf{x}) \cdot \overline{\nabla v}(\mathbf{x})\, d\mathbf{x} &- z \int_D \big(\mathcal{S}\big)_{\beta, z_0}(\mathbf{x}) \overline{v}(\mathbf{x})\, d\mathbf{x} \\
&= \int_D \big(\mathcal{S}\big)_{\beta-1, z_0} \overline{v}(\mathbf{x})\, d\mathbf{x} \quad \forall v \in V,
\end{aligned} \tag{11}
$$

whereas we set $\big(\mathcal{S}\big)_{\beta, z_0} = 0$, whenever $\beta < 0$.

6

Proof. Set $q_\alpha := (Q)_{\alpha, z_0}$ for $\alpha = 0, \ldots, N$. Since

$$(QS)_{\alpha, z_0} = \sum_{n=0}^{\alpha} q_n (S)_{\alpha-n, z_0} = \sum_{n=0}^{N} q_n (S)_{\alpha-n, z_0}$$

according to our convention that $(S)_{\beta, z_0} = 0$ for $\beta < 0$, we have

$$
\begin{aligned}
\bar{j}_{E,\rho}(Q)^2 &= \sum_{\alpha=M+1}^{E} \left\langle (QS)_{\alpha, z_0}, (QS)_{\alpha, z_0} \right\rangle_{V, \sqrt{\mathrm{Re}(z_0)}} \rho^{2\alpha} \\
&= \sum_{\alpha=M+1}^{E} \left\langle \sum_{j=0}^{N} q_j (S)_{\alpha-j, z_0}, \sum_{i=0}^{N} q_i (S)_{\alpha-i, z_0} \right\rangle_{V, \sqrt{\mathrm{Re}(z_0)}} \rho^{2\alpha} \\
&= \sum_{\alpha=M+1}^{E} \sum_{i,j=0}^{N} q_i^* q_j \left\langle (S)_{\alpha-j, z_0}, (S)_{\alpha-i, z_0} \right\rangle_{V, \sqrt{\mathrm{Re}(z_0)}} \rho^{2\alpha} \\
&= \sum_{i,j=0}^{N} q_i^* q_j \sum_{\alpha=M+1}^{E} \left\langle (S)_{\alpha-j, z_0}, (S)_{\alpha-i, z_0} \right\rangle_{V, \sqrt{\mathrm{Re}(z_0)}} \rho^{2\alpha} \\
&= \mathbf{q}^\star G_{E,\rho} \mathbf{q},
\end{aligned}
$$

where $G_{E,\rho} \in \mathbb{C}^{(N+1) \times (N+1)}$ is defined in (10), and $\mathbf{q} = (q_0, \ldots, q_N)^T$. By definition, $G_{E,\rho}$ is Hermitian. Moreover, definition (9) implies that $G_{E,\rho}$ is positive-semidefinite, so that all its eigenvalues are real non-negative. Finally, observe that the constraint $\sum_{\alpha=0}^{N} \left| (Q)_{\alpha, z_0} \right|^2 = 1$ is equivalent to the condition $\|\mathbf{q}\|_2 = 1$. Hence, we conclude that the constrained minimization problem (8) is equivalent to the identification of the (normalized) eigenvector corresponding to the smallest eigenvalue $G_{E,\rho}$. Finally, we observe that equation (11) is obtained by repeated differentiation of equation (2); see [3] for a rigorous derivation. □

The Hermitian matrix $G_{E,\rho}$ defined in (10) is obtained as weighted sum of sub-matrices of the Gram matrix $G \in \mathbb{C}^{(N+1) \times (N+1)}$ associated with the solution map S, namely, the matrix with entries $G_{i,j} = \left\langle (S)_{i, z_0}, (S)_{j, z_0} \right\rangle_{V, \sqrt{\mathrm{Re}(z_0)}}$, for $i, j = 0, \ldots, N$. See Figure 1 for a graphical representation.

By following the steps performed in the proof of Proposition 3.1, and applying Proposition 3.2, we devise Algorithm 1 for the computation of the LS-Padé approximant.

Remark 3.3 *The choice of ρ impacts the algorithm only by determining the weights in the computation of $G_{E,\rho}$. Specifically, small (respectively large) values of ρ emphasize the contributions from the sub-matrices located in the top-left (respectively bottom-right) portion of G. A fast version of the algorithm, where $G_{E,\rho}$ reduces just to the leading term (i.e., for $\rho \to +\infty$), is currently under investigation (see [4]).*

$$G = \begin{bmatrix} \langle \mathcal{S}, \mathcal{S} \rangle_V & \langle \mathcal{S}, \mathcal{S}_1 \rangle_V & \langle \mathcal{S}, \mathcal{S}_2 \rangle_V & \dots & & \\ \langle \mathcal{S}_1, \mathcal{S} \rangle_V & \langle \mathcal{S}_1, \mathcal{S}_1 \rangle_V & \langle \mathcal{S}_1, \mathcal{S}_2 \rangle_V & \langle \mathcal{S}_1, \mathcal{S}_3 \rangle_V & \dots & \\ \langle \mathcal{S}_2, \mathcal{S} \rangle_V & \langle \mathcal{S}_2, \mathcal{S}_1 \rangle_V & \langle \mathcal{S}_2, \mathcal{S}_2 \rangle_V & \langle \mathcal{S}_2, \mathcal{S}_3 \rangle_V & \langle \mathcal{S}_2, \mathcal{S}_4 \rangle_V & \dots \\ \vdots & \langle \mathcal{S}_3, \mathcal{S}_1 \rangle_V & \langle \mathcal{S}_3, \mathcal{S}_2 \rangle_V & \langle \mathcal{S}_3, \mathcal{S}_3 \rangle_V & \langle \mathcal{S}_3, \mathcal{S}_4 \rangle_V & \dots \\ & \vdots & \langle \mathcal{S}_4, \mathcal{S}_2 \rangle_V & \langle \mathcal{S}_4, \mathcal{S}_3 \rangle_V & \langle \mathcal{S}_4, \mathcal{S}_4 \rangle_V & \dots \\ & & \vdots & \vdots & \vdots & \end{bmatrix}$$

$$G_{E,\rho} = \dots + \rho^6 \begin{bmatrix} \langle \mathcal{S}_3, \mathcal{S}_3 \rangle_V & \langle \mathcal{S}_2, \mathcal{S}_3 \rangle_V & \langle \mathcal{S}_1, \mathcal{S}_3 \rangle_V \\ \langle \mathcal{S}_3, \mathcal{S}_2 \rangle_V & \langle \mathcal{S}_2, \mathcal{S}_2 \rangle_V & \langle \mathcal{S}_1, \mathcal{S}_2 \rangle_V \\ \langle \mathcal{S}_3, \mathcal{S}_1 \rangle_V & \langle \mathcal{S}_2, \mathcal{S}_1 \rangle_V & \langle \mathcal{S}_1, \mathcal{S}_1 \rangle_V \end{bmatrix} + \dots$$

Figure 1: Gram matrix (top) associated with the frequency response map $\mathcal{S}$. To lighten the notation, we omit both the argument (z_0) of the Taylor coefficients $\mathcal{S}_\alpha$, and the weight $\sqrt{\mathrm{Re}\,(z_0)}$ of the scalar product $\langle \cdot, \cdot \rangle_V$. In blue the sub-matrix corresponding to $N = 2$ and $\alpha = 3$, which provides a contribution to $G_{E,\rho}$ (bottom) with weight ρ^6. Observe that a transposition with respect to the secondary diagonal is carried out before computing the sum.

Algorithm 1 Construction of the LS-Padé approximant

1: Fix $z_0 \in \mathbb{C} \setminus \Lambda$ with $\mathrm{Re}\,(z_0) > 0$, $\rho \in \mathbb{R}^+$, M, N, $E \in \mathbb{N}$, with $E \geq M + N$
2: Evaluate $\mathcal{S}$ in the center z_0, by solving problem (2)
3: **for** $\beta = 1, \dots, E$ **do**
4:     Compute the Taylor coefficient of $\mathcal{S}$ in z_0 of order β, $\left(\mathcal{S} \right)_{\beta, z_0}$, by solving the problem (11)
5: **end for**
6: Define the matrix $G_{E,\rho} \in \mathbb{R}^{(N+1) \times (N+1)}$ according to (10)
7: Compute the (normalized) eigenvector $\xi = (\xi_0, \dots, \xi_N)$ corresponding to the smallest non-negative eigenvalue of the matrix $G_{E,\rho}$
8: Define the denominator as $\mathcal{Q}_{[M/N]}(z) = \sum_{\alpha=0}^{N} \xi_\alpha (z - z_0)^\alpha$
9: **for** $\alpha = 0, \dots, N$ **do**
10:     Compute the Taylor coefficient of $\mathcal{S}\mathcal{Q}_{[M/N]}$ in z_0 of order α using the formula $\left(\mathcal{S}\mathcal{Q}_{[M/N]} \right)_{\alpha, z_0} = \sum_{n=0}^{\alpha} \xi_n \left(\mathcal{S} \right)_{\alpha - n, z_0}$
11: **end for**
12: Define the numerator as $\mathcal{P}_{[M/N]}(z) = \sum_{\alpha=0}^{M} \left(\mathcal{S}\mathcal{Q}_{[M/N]} \right)_{\alpha, z_0} (z - z_0)^\alpha$
13: Define the single-point LS-Padé approximant as $\mathcal{S}_{[M/N]} = \frac{\mathcal{P}_{[M/N]}}{\mathcal{Q}_{[M/N]}}$

---

4   Application to a transmission/reflection problem

We consider the transmission/reflection problem treated in [18], i.e., the transmission/reflection of a plane wave $e^{i\kappa \mathbf{x} \cdot \mathbf{d}}$ with wavenumber κ and direction $\mathbf{d} = (\cos(\theta), \sin(\theta))$, across a fluid-fluid interface. In particular, the considered domain $D = (-1, 1)^2$ is divided into two regions with different refractive indices n_1, n_2; we assume $n_1 < n_2$. The Helmholtz problem is the following

$$-\Delta u - \kappa^2 \varepsilon_r^2 u = 0, \quad \text{with } \varepsilon_r(x_1, x_2) = \begin{cases} n_1 & \text{if } x_2 < 0, \\ n_2 & \text{if } x_2 > 0. \end{cases} \quad (12)$$

For any angle $0 \leq \theta < \pi/2$, the following function is a solution of equation (12):

$$u_{ex}(x_1, x_2) = \begin{cases} T \exp\{i\mathbf{K} \cdot \mathbf{x}\} & \text{if } x_2 > 0, \\ \exp\{i\kappa n_1 \mathbf{d} \cdot \mathbf{x}\} + R \exp\{i\kappa n_1 \mathbf{d} \cdot (x_1, -x_2)\} & \text{if } x_2 < 0. \end{cases} \quad (13)$$

where $\mathbf{K} = (\kappa n_1 d_1, \kappa \sqrt{n_2^2 - (n_1 d_1)^2})$, $R = -\frac{K_2 - \kappa n_1 d_2}{K_2 + \kappa n_1 d_2}$ and $T = 1 + R$. We couple the Helmholtz equation (12) with Dirichlet boundary conditions derived from the exact solution (13), i.e., $u|_{\partial D} = u_{ex}|_{\partial D}$.

Depending on the value of θ (angle of the incident wave), the solution may exhibit two types of behavior:

- if $\theta < \theta_{crit} := \arccos\left(\frac{n_2}{n_1}\right)$, then $\text{Im}(K_2) \neq 0$, and u_{ex} decays exponentially for $x_2 > 0$. Physically, this phenomenon is called *total internal reflection*;

- if $\theta > \theta_{crit}$, then $\mathbf{d}$ is close to the normal incidence, and the wave is *refracted* at the interface.
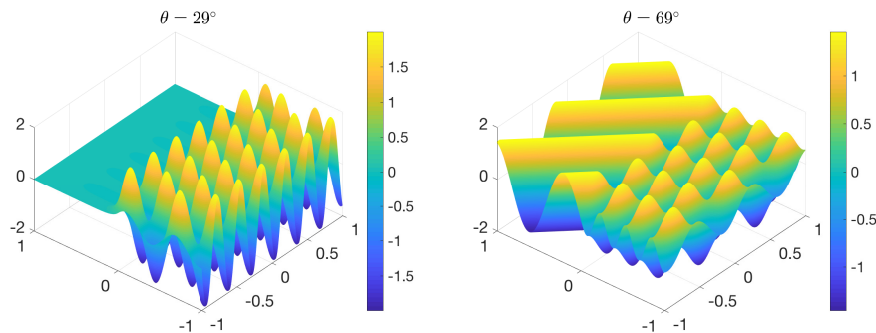
The two behaviors are depicted in Figure 2.

Figure 2: Exact solution of the transmission/reflection problem with $n_1 = 2$, $n_2 = 1$, $\kappa = 11$ and $\theta = 29°$ (left), $\theta = 69°$ (right).

4.1   Frequency response map

We are interested in the following boundary value problem:

Problem 2 (Transmission/Reflection Problem) *The wavenumber κ^2 ranges in the interval of interest $K = [\kappa_{min}^2, \kappa_{max}^2]$, and the Helmholtz equation is endowed with Dirichlet boundary conditions on $\Gamma_D = \partial D$:*

$$\begin{cases} -\Delta u - \kappa^2 \varepsilon_r^2 u = 0 & in \ D, \\ u = g_D & on \ \partial D, \end{cases} \tag{14}$$

where $g_D := u_{ex}|_{\partial D}$, and u_{ex} is given by formula (13) with $\kappa = 11$ and either $\theta = 29°$ or $\theta = 69°$.

A weak formulation of problem (14) with $z \in \mathbb{C}$ replacing κ^2 reads: find $\mathring{u} \in V = H_0^1(D)$ such that

$$\int_D \nabla \mathring{u}_z(\mathbf{x}) \cdot \overline{\nabla v}(\mathbf{x}) d\mathbf{x} - z \int_D \varepsilon_r^2(\mathbf{x}) \mathring{u}_z(\mathbf{x}) \overline{v}(\mathbf{x}) d\mathbf{x}$$

$$= z \int_D \varepsilon_r^2(\mathbf{x}) w_g(\mathbf{x}) \overline{v}(\mathbf{x}) d\mathbf{x} \quad \forall v \in V, \tag{15}$$

where $w_g \in H^1(D)$ is the unique harmonic extension of g_D, i.e., $\Delta w_g = 0$ in D and $w_g|_{\partial D} = g_D$, and $\mathring{u} := u - w_g$.

By generalizing [3, Theorem 2.1], it can be proved that problem (15) admits a unique solution for all $z \in \mathbb{C} \setminus \Lambda$, Λ being the set of eigenvalues of the Laplacian (w.r.t. the weighted $L^2(D)$-norm $\|v\|_{L^2(D),\varepsilon_r} = \|\varepsilon_r v\|_{L^2(D)}$) with homogeneous Dirichlet boundary conditions. Moreover, with

$$0 < \alpha < \min_{j:\lambda_j \in \Lambda} |\lambda_j - z|, \tag{16}$$

the unique solution satisfies the a priori bound

$$\|\mathring{u}_z\|_{V,\sqrt{\mathrm{Re}(z_0)}} \leq \max\{1, n_1, n_2\} \frac{\sqrt{|\lambda_{min} - z| + |\mathrm{Re}\,(z)| + \mathrm{Re}\,(z_0)}}{\alpha} |z| \|w_g\|_{L^2(D)}, \tag{17}$$

where $\lambda_{min} := \min\{\lambda \in \Lambda\}$. By triangular inequality, an analogous upper bound on $\|u_z\|_{V,\sqrt{\mathrm{Re}(z_0)}}$ follows.

Let us denote by $\mathcal{S} : \mathbb{C} \to V := H^1(D)$ the frequency response map that associates to each complex wavenumber z, the function $\mathcal{S}(z) = \mathring{u}_z + w_g$, with $\mathring{u}_z$ the weak solution of (15).

Proposition 4.1 *The frequency response map $\mathcal{S}$ is meromorphic in $\mathbb{C}$, having a pole of order one in each $\lambda \in \Lambda$, where Λ is the set of eigenvalues of the Laplacian (w.r.t. the weighted $L^2(D)$-norm $\|\cdot\|_{L^2(D),\varepsilon_r}$) with homogeneous Dirichlet boundary conditions.*

Proof. We denote with $\langle \cdot, \cdot \rangle_{\varepsilon_r}$ the inner product which induces the $L^2(D)$ weighted norm $\|\cdot\|_{L^2(D),\varepsilon_r}$, i.e., $\langle v_1, v_2 \rangle_{\varepsilon_r} := \int_D \varepsilon_r^2(\mathbf{x}) v_1(\mathbf{x}) v_2(\mathbf{x}) d\mathbf{x}$. Let $\{\varphi_j\}$ be the set of eigenfunctions of the Laplacian (with homogeneous Dirichlet boundary conditions) orthonormal with respect to the inner product $\langle \cdot, \cdot \rangle_{\varepsilon_r}$, and let $\{\lambda_j\}$ be the corresponding eigenvalues, i.e., $-\Delta \varphi_j = \lambda_j \varepsilon_r^2 \varphi_j$ in D and $\varphi_j|_{\partial D} = 0$ (see, e.g., [21, Theorem 2.36]). Inserting into equation (15) the eigenfunction expansion $\mathring{u}(z, \mathbf{x}) = \sum_j \mathring{u}_j(z) \varphi_j(\mathbf{x})$, where $\mathring{u}_j(z) := \langle \mathring{u}(z), \varphi_j \rangle_{\varepsilon_r}$, and denoting $w_j := \langle w_g, \varphi_j \rangle_{\varepsilon_r}$, we derive

$$\mathring{u}_j(z) = \frac{z \, w_j}{\lambda_j - z}. \tag{18}$$

The eigenfunction expansion of the frequency response map is then given by

$$\mathcal{S}(z) = \mathring{u}(z, \mathbf{x}) + w_g(\mathbf{x}) = \sum_j \mathring{u}_j(z) \varphi_j(\mathbf{x}) + w_g(\mathbf{x})$$

$$\overset{(18)}{=} \sum_j \frac{z w_j}{\lambda_j - z} \varphi_j(\mathbf{x}) + w_g(\mathbf{x}). \tag{19}$$

Since the series converges in the (weighted) $H^1(D)$-norm, then (19) directly implies that $\mathcal{S}$ is meromorphic in $\mathbb{C}$, and each $\lambda \in \Lambda$ is a pole of order one for $\mathcal{S}$. □

4.2 LS-Padé approximant of the frequency response map

Since the frequency response map is meromorphic, it is appropriate to use the LS-Padé technology to catch the singularities of $\mathcal{S}$, and provide sharp approximations of $\mathcal{S}(z)$, when z is close to the center z_0. We apply Algorithm 1, and compute the coefficients of the denominator as the entries of the eigenvector corresponding to the minimal eigenvalue of the Gram matrix (10). The Taylor coefficient of order $\beta \geq 1$, $(\mathcal{S})_{\beta,z_0} = \frac{1}{\beta!} \frac{d^\beta \mathcal{S}}{dz^\beta}|_{z=z_0} \in H^1_0(D)$, satisfies

$$
\int_D \nabla(\mathcal{S})_{\beta,z_0}(\mathbf{x}) \cdot \overline{\nabla v}(\mathbf{x}) d\mathbf{x} - z_0 \int_D \varepsilon_r^2(\mathbf{x})(\mathcal{S})_{\beta,z_0}(\mathbf{x})\overline{v}(\mathbf{x}) d\mathbf{x}
$$
$$
= \int_D \varepsilon_r^2(\mathbf{x})(\mathcal{S})_{\beta-1,z_0}(\mathbf{x})\overline{v}(\mathbf{x}) d\mathbf{x} \quad \forall v \in H^1_0(D). \tag{20}
$$

Problem (20) admits a unique solution for all $z \in \mathbb{C} \setminus \Lambda$, since the PDE operator is the same as in (15) and the right-hand side is a bounded linear form.

Let $K = [3, 12]$ be the interval of interest and $\theta = 29°$. In Figure 3, the $H^1(D)$-weighted norm of the $\mathbb{P}^2$ finite element approximation of $\mathcal{S}$, $\mathcal{S}_h$, is compared with the norm of its LS-Padé approximant $\mathcal{S}_{h,P}$ centered in $z_0 = 7.5 + 0.5i$, for various degrees (M, N). We have empirically observed (see Figure 4) that the LS-Padé approximation delivers a better accuracy than that predicted in (7):

$$
\left\| \mathcal{S}_h(z) - \mathcal{S}_{[M/N],h}(z) \right\|_{V, \sqrt{\mathrm{Re}(z_0)}} \sim \left(\frac{|z_0 - z|}{|z_0 - \lambda_{N+1}|} \right)^{M+1}, \tag{21}
$$

where $\{\lambda_j\}_j$ are the elements of Λ ordered according to: $|\lambda_1 - z_0| < |\lambda_2 - z_0| < \ldots$. We refer to [4] for a formal derivation of (21), where $\mathcal{S}_{[M/N]}$ is computed by a fast version of Algorithm 1.
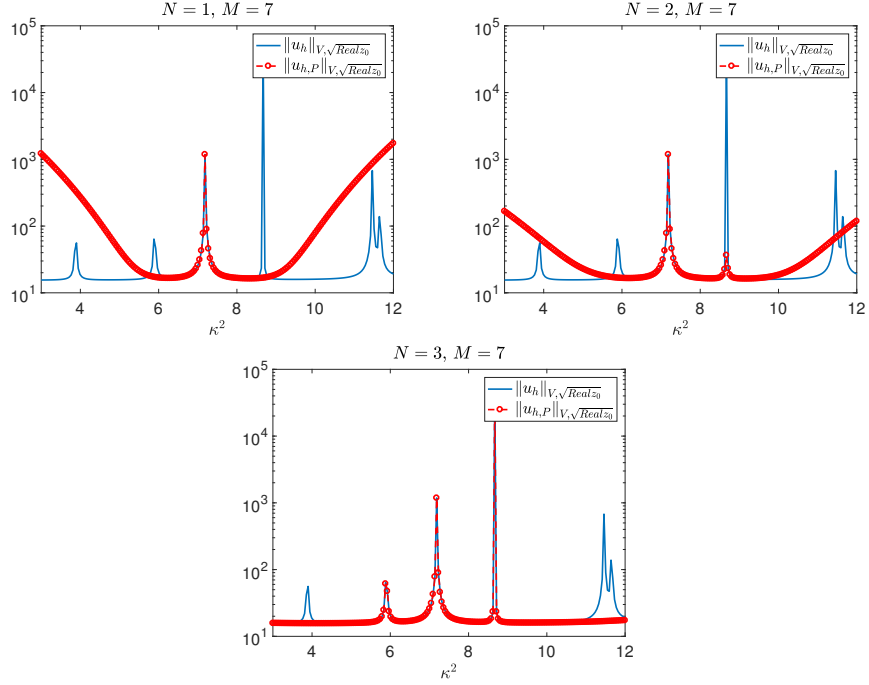
Figure 3: Comparison between the $H^1(D)$-weighted norm of $\mathcal{S}_h$ (with $\theta = 29°$) and of its LS-Padé approximant $\mathcal{S}_{h,P}$ centered in $z_0 = 7.5 + 0.5i$.
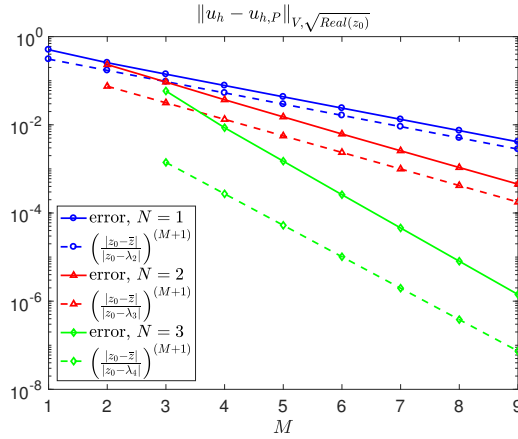

Figure 4: LS-Padé approximation error, compared with the heuristic slope $\left(\frac{|z_0 - \bar{z}|}{|z_0 - \lambda_{N+1}|}\right)^{M+1}$ for $\bar{z} = 8$.

5 Application to a scattering problem

In this section, we consider the scattering of an acoustic wave at a scatter occupying the domain $\mathcal{B}((0,0),0.5) \subset \mathbb{R}^2$. The incident wave u^i is the time-harmonic plane wave traveling along the direction $\mathbf{d} = (\cos(\theta), \sin(\theta))$ with wavenumber k, i.e., $u^i = e^{ik\mathbf{d}\cdot\mathbf{x}}$. The total field u, given by the sum of the incident wave u^i with the scattered wave u^s, satisfies the following boundary value problem in the infinite domain $\mathbb{R}^2 \setminus \mathcal{B}((0,0),0.5) \subset \mathbb{R}^2$

$$\begin{cases} -\Delta u - k^2 u = 0 & \text{in } \mathbb{R}^2 \setminus \overline{\mathcal{B}((0,0),0.5) \subset \mathbb{R}^2}, \\ u = 0 & \text{on } \Gamma_D := \partial\mathcal{B}((0,0),0.5) \subset \mathbb{R}^2, \\ \lim_{|\mathbf{x}|\to\infty} |x|^{1/2} \left(\frac{\partial u^s(\mathbf{x})}{\partial|x|} - iku^s(\mathbf{x}) \right) = 0 \end{cases} \quad (22)$$

The finite element approximation of problem (22) entails the truncation of the unbounded domain $\mathbb{R}^2 \setminus \overline{\mathcal{B}((0,0),0.5) \subset \mathbb{R}^2}$ into the bounded domain

$$D := ([-2,2] \times [-2,2]) \setminus \overline{\mathcal{B}(0,0.5)},$$

whose outer boundary will be denoted as Γ_R. Approximating the Sommerfeld radiation condition at infinity in problem (22) by a first order absorbing boundary condition, we write the following parametric problem:

Problem 3 (Scattering Problem) *The wavenumber k^2 ranges in the interval of interest $K := [k_{min}^2, k_{max}^2] \subset \mathbb{R}^+$, $\mathbf{n}$ is the outgoing normal vector field to Γ_R, and $g_R := \frac{\partial u^i}{\partial \mathbf{n}} - iku^i$ is the impedance trace of the incoming wave u^i. We consider the Helmholtz boundary value problem*

$$\begin{cases} -\Delta u - k^2 u = 0 & \text{in } D, \\ u = 0 & \text{on } \Gamma_D, \\ \frac{\partial u}{\partial \mathbf{n}} - iku = g_R & \text{on } \Gamma_R. \end{cases} \quad (23)$$

5.1 Regularity of the frequency response map

We extend problem (23) to complex wavenumbers. Given a complex wavenumber $z \in \mathbb{C}$, we introduce the incident plane wave $u^i = e^{iz\mathbf{d}\cdot\mathbf{x}}$ and its impedance trace $g_z := \frac{\partial u^i}{\partial \mathbf{n}} - izu^i$, and we define the frequency response map $\mathcal{S} : z \mapsto \mathcal{S}(z) := u_z \in V := H^1_{\Gamma_D}(D)$, where u_z satisfies

$$\int_D \nabla u_z(\mathbf{x}) \cdot \overline{\nabla v}(\mathbf{x}) d\mathbf{x} - z^2 \int_D u_z(\mathbf{x})\overline{v}(\mathbf{x}) d\mathbf{x} - iz \int_{\Gamma_R} u_z(\mathbf{x})\overline{v}(\mathbf{x}) ds \quad (24)$$

$$= \int_{\Gamma_R} g_z(\mathbf{x})\overline{v}(\mathbf{x}) ds \quad \forall \, v \in V.$$

If $z \in \mathbb{R}$, problem (24) admits a unique solution (see, e.g., [11]), which implies that the frequency response map is well-defined on $\mathbb{R}$. The following Theorem extends this result to the complex half plane $\{z \in \mathbb{C} : \text{Im}(z) \geq 0\}$. Since the wavenumber in (24) is square of the parameter z, we will endow the Hilbert space V with the weighted $H^1(D)$-norm, with weight $w = \text{Re}(z_0)$ (and not $w = \sqrt{\text{Re}(z_0)}$, as was done before).

Theorem 5.1 *Problem (24) admits a unique solution in all compact subsets of*

$$\mathbb{C}^+ := \{z \in \mathbb{C} : \text{Im}(z) \geq 0\}. \quad (25)$$

Proof. Given $z \in \mathbb{C}$, we introduce the bilinear and linear forms which define problem (24):

$$B_z(u,v) := \int_D \nabla u_z(\mathbf{x}) \cdot \overline{\nabla v}(\mathbf{x}) d\mathbf{x} - z^2 \int_D u_z(\mathbf{x}) \overline{v}(\mathbf{x}) d\mathbf{x} - iz \int_{\Gamma_R} u_z(\mathbf{x}) \overline{v}(\mathbf{x}) ds, \qquad (26)$$

$$L_z(v) := \int_{\Gamma_R} g_z(\mathbf{x}) \overline{v}(\mathbf{x}) ds. \qquad (27)$$

We first show that either the coercivity or the Gårding inequality (see [21]) holds, provided that $\text{Im}(z)$ is non-negative. For the bilinear form in (26), we have

$$\begin{aligned}
\text{Re}(B_z(u,u)) &= \|\nabla u\|_{L^2(D)}^2 - (\text{Re}(z)^2 - \text{Im}(z)^2) \|u\|_{L^2(D)}^2 + \text{Im}(z) \|u\|_{L^2(\Gamma_R)}^2 \\
&\geq \|\nabla u\|_{L^2(D)}^2 - (\text{Re}(z)^2 - \text{Im}(z)^2) \|u\|_{L^2(D)}^2 \\
&= \|u\|_{V,\text{Re}(z_0)}^2 - (\text{Re}(z)^2 - \text{Im}(z)^2 + \text{Re}(z_0)^2) \|u\|_{L^2(D)}^2.
\end{aligned}$$

If $C := \text{Re}(z)^2 - \text{Im}(z)^2 + \text{Re}(z_0)^2 \leq 0$, then $B(\cdot,\cdot)$ is coercive, whereas if $C > 0$, then $B_z(\cdot,\cdot)$ satisfies the Gårding inequality.

The bilinear form (26) is bounded, with constant $C = \max\left\{1, \frac{|z|^2}{\text{Re}(z_0)}, \frac{|z| C_{tr}^2}{\text{Re}(z_0)}\right\}$. Indeed, using the trace inequality

$$\|u\|_{L^2(\Gamma_R)} \leq C_{tr} \|u\|_{H^1(D)},$$

we get

$$\begin{aligned}
|B_z(u,v)| &\leq \|\nabla u\|_{L^2(D)} \|\nabla v\|_{L^2(D)} + |z|^2 \|u\|_{L^2(D)} \|v\|_{L^2(D)} + |z| \|u\|_{L^2(\Gamma_R)} \|v\|_{L^2(\Gamma_R)} \\
&\leq \|\nabla u\|_{L^2(D)} \|\nabla v\|_{L^2(D)} + |z|^2 \|u\|_{L^2(D)} \|v\|_{L^2(D)} + |z| C_{tr}^2 \|u\|_{H^1(D)} \|v\|_{H^1(D)} \\
&\leq \|\nabla u\|_{L^2(D)} \|\nabla v\|_{L^2(D)} + \frac{|z|^2 \text{Re}(z_0)^2}{\text{Re}(z_0)^2} \|u\|_{L^2(D)} \|v\|_{L^2(D)} \\
&\quad + |z| C_{tr}^2 \max\left\{1, \frac{1}{\text{Re}(z_0)^2}\right\} \|u\|_{V,\text{Re}(z_0)} \|v\|_{\text{Re}(z_0)} \\
&\leq \max\left\{1, \frac{|z|^2}{\text{Re}(z_0)^2}, \frac{|z| C_{tr}^2}{\text{Re}(z_0)^2}\right\} \|u\|_{V,\text{Re}(z_0)} \|v\|_{\text{Re}(z_0)}.
\end{aligned}$$

Moreover, the linear functional (27) is bounded, with constant

$$C = C_{tr}^2 \max\left\{1, \frac{1}{\text{Re}(z_0)^2}\right\} \|g_z\|_{V,\text{Re}(z_0)}.$$

Problem (24) admits a unique solution (continuously dependent on the data) if and only if its homogeneous adjoint problem admits only trivial solutions: see [21, Theorem 4.11]. We consider the case $\text{Im}(z) > 0$, and we refer to [11] for $\text{Im}(z) = 0$. The bilinear form associated with the adjoint problem with $g_z = 0$ reads:

$$B_z^*(\varphi,v) := \overline{B_z(v,\varphi)} = \int_D \nabla \varphi(\mathbf{x}) \cdot \overline{\nabla v}(\mathbf{x}) d\mathbf{x} - \overline{z}^2 \int_D \varphi(\mathbf{x}) \overline{v}(\mathbf{x}) d\mathbf{x} - \overline{iz} \int_{\Gamma_R} \varphi(\mathbf{x}) \overline{v}(\mathbf{x}) ds,$$

and the condition $B_z^*(u,u) = 0$ is equivalent to

$$\begin{cases}
\text{Re}(B_z^*(u,u)) = \|\nabla u\|_{L^2(D)}^2 - (\text{Re}(z)^2 - \text{Im}(z)^2) \|u\|_{L^2(D)}^2 + \text{Im}(z) \|u\|_{L^2(\Gamma_R)}^2 = 0 \\
\text{Im}(B_z^*(u,u)) = \text{Re}(z) \left(2\text{Im}(z) \|u\|_{L^2(D)}^2 + \|u\|_{L^2(\Gamma_R)}^2\right) = 0
\end{cases}$$

If $\text{Re}(z) \neq 0$ and $\text{Im}(z) > 0$, then $\text{Im}(B_z^*(u,u)) = 0$ is equivalent to $\|u\|_{L^2(D)} = \|u\|_{L^2(\Gamma_R)} = 0$, that is, $u = 0$ in D, whereas, if $\text{Re}(z) = 0$ and $\text{Im}(z) > 0$, then $\text{Re}(B_z^*(u,u)) = 0$ implies $\|\nabla u\|_{L^2(D)} = \|u\|_{L^2(D)} = \|u\|_{L^2(\Gamma_R)} = 0$, hence $u = 0$. $\qquad \square$

We recall here the following theorem, see [27, Theorem 1], which will be used in the proof of Proposition 5.3.

Theorem 5.2 *Let B be an open and connected subset of the complex plane. If $\{T(z)\}_{z \in B}$ is an analytic family of compact operators defined on a given Banach space, then either $(I - T(z))$ is nowhere invertible in B or $(I - T(z))^{-1}$ is meromorphic in B.*

Proposition 5.3 *The frequency response map $\mathcal{S}$ associated with problem (24) is meromorphic in all open bounded and connected subsets of $\mathbb{C}$, and all its poles have negative imaginary part.*

Proof. We proceed as in [20, Proposition 2]. We add and subtract the term $\int_D u_z \overline{v} dx$ to the left-hand side of (24), and we get

$$\int_D \nabla u_z(\mathbf{x}) \cdot \overline{\nabla v}(\mathbf{x}) d\mathbf{x} + \int_D u_z(\mathbf{x}) \overline{v}(\mathbf{x}) dx - (1 + z^2) \int_D u_z(\mathbf{x}) \overline{v}(\mathbf{x}) d\mathbf{x}$$
$$- iz \int_{\Gamma_R} u_z(\mathbf{x}) \overline{v}(\mathbf{x}) ds = \int_{\Gamma_R} g_z(\mathbf{x}) \overline{v}(\mathbf{x}) ds \quad \forall v \in V,$$

which can be written equivalently as

$$(I - T(z))u_z = G_z \quad \text{in } V, \tag{28}$$

where $T(z), G_z : V \to V$ are defined, respectively, as

$$\langle T(z)u, v \rangle_V = (1 + z^2) \int_D u(\mathbf{x}) \overline{v}(\mathbf{x}) d\mathbf{x} + iz \int_{\Gamma_R} u(\mathbf{x}) \overline{v}(\mathbf{x}) ds \quad \forall v \in V,$$

$$\langle G_z, v \rangle_V = \int_{\Gamma_R} g_z \overline{v}(\mathbf{x}) ds \quad \forall v \in V.$$

Therefore, $\mathcal{S}(z) = (I - T(z))^{-1} G_z$. We prove that $T(z)$ is compact in all open bounded connected subsets of the complex plane $\mathbb{C}$. We write $T(z)$ as $T(z) = \widetilde{T}(z) \circ J$, where J is the compact embedding $J : V \to H^{1/2+\varepsilon}(D)$, and $\widetilde{T}(z) : H^{1/2+\varepsilon}(D) \to V$. Hence, in order to prove the compactness of $T(z)$, it is enough to show that $\widetilde{T}(z)$ is continuous. For all $u \in H^{1/2+\varepsilon}(D)$, we have

$$\left\| \widetilde{T}(z)u \right\|_V = \sup_{v \in V, \|v\|_V = 1} \left| \left\langle \widetilde{T}(z)u, v \right\rangle_V \right|$$

$$= \sup_{v \in V, \|v\|_V = 1} \left| (1 + z^2) \int_D u(\mathbf{x}) \overline{v}(\mathbf{x}) d\mathbf{x} + iz \int_{\Gamma_R} u(\mathbf{x}) \overline{v}(\mathbf{x}) ds \right|$$

$$\leq \sup_{\|v\|_V = 1} \left(|1 + z^2| \|u\|_{L^2(D)} \|v\|_{L^2(D)} + |z| \|u\|_{L^2(\Gamma_R)} \|v\|_{L^2(\Gamma_R)} \right)$$

$$\leq \sup_{\|v\|_V = 1} \left(|1 + z^2| \|u\|_{L^2(D)} \|v\|_{L^2(D)} + |z| \|u\|_{L^2(\partial D)} \|v\|_{L^2(\partial D)} \right)$$

$$\leq \sup_{\|v\|_V = 1} \left(|1 + z^2| \|u\|_{L^2(D)} \|v\|_{L^2(D)} + C_{tr}^2 |z| \|u\|_{H^{1/2+\varepsilon}(D)} \|v\|_{H^{1/2+\varepsilon}(D)} \right)$$

$$\leq \max\{ |1 + z^2|, C_{tr}^2 |z| \} \|u\|_{H^{1/2+\varepsilon}(D)},$$

where C_{tr} is the continuity constant of the trace operator $\gamma : H^{1/2+\varepsilon}(D) \to L^2(\partial D)$ (see, e.g., [1, Theorem 5.36]). Applying Theorem 5.2, we conclude that $(I - T(z))^{-1}$ is meromorphic in all open bounded and connected subsets of $\mathbb{C}$ and, since G_z is linear in z (hence holomorphic in $\mathbb{C}$), the same conclusion applies to the frequency response function $\mathcal{S}(z) = (I - T(z))^{-1} G_z$. Moreover, since Theorem 5.1 states that $\mathcal{S}$ is well defined in $\mathbb{C}^+$, we deduce that all poles of $\mathcal{S}$ must have negative imaginary part. $\qquad\square$

5.2 LS-Padé approximant of the frequency response map

We construct the LS-Padé approximant of the frequency response map $\mathcal{S}$ following Algorithm 1. Having fixed $z_0 \in \mathbb{C}^+$, N, M, and $E \geq M + N$, the coefficients of the denominator are computed by identifying the eigenvector corresponding to the smallest eigenvalue of the matrix (10), where the β-th Taylor coefficient of $\mathcal{S}$, $(\mathcal{S})_{\beta,z_0}$, solves the following recursive problem:

$$\int_D \nabla (\mathcal{S})_{\beta,z_0}(\mathbf{x}) \cdot \overline{\nabla v}(\mathbf{x})d\mathbf{x} - z_0^2 \int_D (\mathcal{S})_{\beta,z_0}(\mathbf{x})\overline{v}(\mathbf{x})d\mathbf{x} - iz_0 \int_{\Gamma_R} (\mathcal{S})_{\beta,z_0}(\mathbf{x})\overline{v}(\mathbf{x})ds$$

$$= 2z_0 \int_D (\mathcal{S}(\mathbf{x}))_{\beta-1,z_0}\overline{v}(\mathbf{x})d\mathbf{x} + i \int_{\Gamma_R} (\mathcal{S}(\mathbf{x}))_{\beta-1,z_0}\overline{v}(\mathbf{x})ds$$

$$+ \int_D (\mathcal{S}(\mathbf{x}))_{\beta-2,z_0}\overline{v}(\mathbf{x})d\mathbf{x} + \frac{1}{\beta!}\int_{\Gamma_R} \frac{d^\beta}{dz}g_z(\mathbf{x})|_{z=z_0} \cdot \overline{v}(\mathbf{x})ds \quad \forall \, v \in V. \tag{29}$$

Since the PDE operator in (29) is the same as in (24), and the linear form at the right-hand side is bounded, by applying Theorem 5.1, we conclude that problem (29) is well-posed for any $z \in \mathbb{C}^+$.
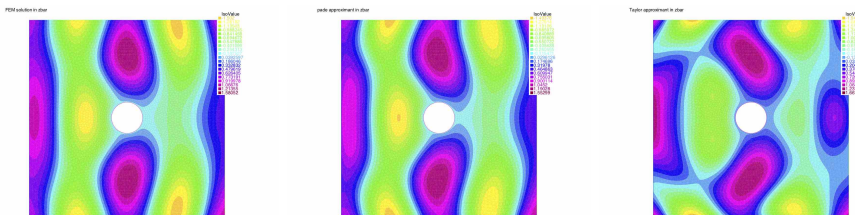

Figure 5: Comparison between the $\mathbb{P}^3$ finite element solution of problem (24) (left), with its LS-Padé approximation $\mathcal{S}_{[M/N]}(z)$ centered in $z_0 = 3 + 0.5i$ with degree $(M,N) = (10,2)$ (center), and its Taylor polynomial centered in $z_0 = 3 + 0.5i$ with degree $M+N = 12$ (right), in the point $z = 2$.

Let u^i be the incident wave traveling along the direction $\mathbf{d} = (\cos(0), \sin(0))$ with wavenumber $z = 2$. Figure 5 (left) represents the solution of problem (24) computed via the finite element method with polynomials of degree 3. Figure 5 (center) and (right) represents the LS-Padé approximation $\mathcal{S}_{[M/N]}(z)$ at $z = 2$ with center $z_0 = 3 + 0.5i$ and degree $(M,N) = (10,2)$ (and parameters $\rho = |z - z_0|$, $E = M + N$), and the Taylor polynomial centered in $z_0 = 3 + 0.5i$ with degree $E = 12$, respectively. Both the Padé and the Taylor approximant are constructed starting from the set of evaluations $\{\mathcal{S}(z_0), (\mathcal{S})_1(z_0), \ldots, (\mathcal{S})_{12}(z_0)\}$. The LS-Padé approximant reproduces the behavior of the reference solution much better than the Taylor approximant, and the LS-Padé relative error in the weighted $H^1(D)$-norm $err_{pade} = 0.101089$ is much smaller than the Taylor one $err_{tay} = 0.611428$.

Let $z = 3$, and $z_0 = 3 + 0.5i$. In Figure 6 (left) we plot the relative LS-Padé approximation error versus the degree of the LS-Padé numerator, for different values of denominator degree. In Figure 6 (right), the relative error obtained by approximating the frequency response map with the Taylor polynomial (black dashed line), and with the LS-Padé approximant are compared. Also the diagonal LS-Padé approximant is considered (dashed purple line), where the LS-Padé numerator and denominator have the same degree. In Figure 6 (right), the errors are plotted versus the number of derivatives $(\mathcal{S})_{\beta,z_0}$, $\beta = 0, \ldots, E$ computed (i.e., the number of PDEs solved offline). Since

$\mathcal{B}(z_0, |z - z_0|)$, the disk with center $z_0 = 3 + 0.5i$ and radius $r_1 = |z - z_0| = 0.5$, is contained in the half plane where the frequency response map is holomorphic (see Proposition 5.3), the Taylor series centered in z_0 converges, and the Taylor approximation error is comparable to the LS-Padé approximation error. Figure 7 presents analogous plots as in Figure 6, for the point $z = 2$. In this case, $\mathcal{B}(z_0, |z - z_0|) \cap \{\operatorname{Im}(z) < 0\} \neq \emptyset$, and the Taylor series diverges.
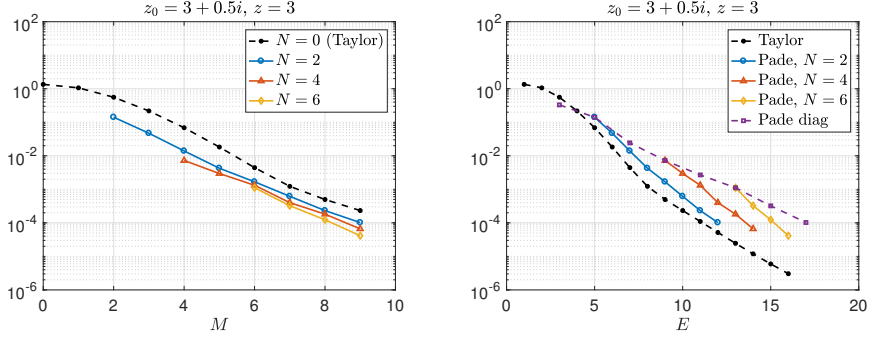
Figure 6: Relative Taylor and LS-Padé approximation error in $z = 3$ plotted versus the numerator degree (left), and the number of derivatives $(\mathcal{S})_{\beta, z_0}$, $\beta = 0, \ldots, E$ computed offline (right).
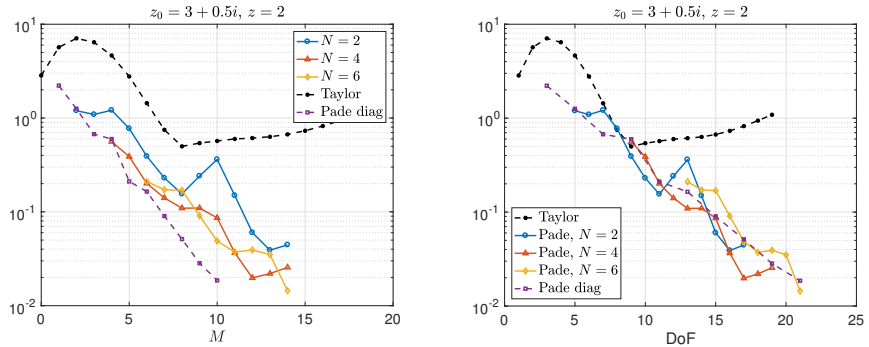
Figure 7: Relative Taylor and LS-Padé approximation error in $z = 2$ plotted versus the numerator degree (left), and the number of derivatives $(\mathcal{S})_{\beta, z_0}$, $\beta = 0, \ldots, E$ computed offline (right).

6 Application in high frequency regime

In this section, we want to study the approximation properties of the LS-Padé approximant in the high frequency regime. As in [3], we consider Problem (1) with $D = (0, \pi) \times (0, \pi)$, $\Gamma_D = \partial D$, $g_D = 0$, and $f(\mathbf{x}) = -\Delta w(x) - \nu^2 w(x)$, where $w(x)$ is the product between the plane wave $e^{-i\nu \mathbf{d} \cdot \mathbf{x}}$ with wavenumber $\nu = \sqrt{51}$ traveling along the direction $\mathbf{d} = (\cos(\pi/6), \sin(pi/6))$ and the normalized quadratic bubble function vanishing on ∂D. Note that $w(x)$ is the exact solution of the Helmholtz equation (2), i.e.,

17

$\mathcal{S}(z) = w$, when $z = \nu^2$. The interval of frequencies we are interested in is $K = [39, 55]$, which contains 6 eigenvalues of the Dirichlet-Laplace operator: $40, 41, 45, 50, 52, 53$.

In Figure 8, we plot the numerical solution $\mathcal{S}_h \in V$ of problem (2) with $z = 51$, computed via $\mathbb{P}^3$ continuous finite elements. Observe that the relative finite element error is of the order of 10^{-5}. In Figure 9, the LS-Padé approximant $\mathcal{S}_{h,P}$ centered in $z_0 = 47 + 0.5i$ evaluated in $z = 51$ is represented for two different values of the denominator degree. Due to the fact that more derivatives are employed in the right plot, more accurate results are obtained with higher denominator polynomial degrees.

In Figure 10, we plot the LS-Padé approximation error w.r.t. the exact solution, in $z = 51$, for different values of the degree of the denominator, and we compare it with the numerical rate (21). When $N = 2, 4$, the LS-Padé technique works as expected (or even better), whereas for $N = 6$ the error is no longer decreasing. We believe that this behavior is caused by the ill-conditioning of Step 7 in Algorithm 1), i.e., the computation of the (normalized) eigenvector of the Gramian matrix $G_{E,\rho}$ defined in (10).

We partition uniformly the interval of interest K in 100 subintervals. At each point z of the grid we have computed the numerical solution $\mathcal{S}_h(z)$ of the Helmholtz problem (2), and the LS-Padé approximant $\mathcal{S}_{h,P}$ (see Figure 11), as well as the relative error $\frac{\|\mathcal{S}_h(z) - \mathcal{S}_{h,P}(z)\|_{H^1(D),\sqrt{\mathrm{Re}(z_0)}}}{\|\mathcal{S}_h(z)\|_{H^1(D),\sqrt{\mathrm{Re}(z_0)}}}$ (see Figure 12). In Figure 13, we study the convergence of the roots of the LS-Padé denominator $\mathcal{Q}_{[M/N]}$ to the exact Laplace eigenvalues. For all degrees of the LS-Padé denominator $\mathcal{Q}_{[M/N]}$, there are two roots of $\mathcal{Q}_{[M/N]}$ which converge to the two Laplace eigenvalues closest to z_0. Concerning the other roots, we observe two regimes: the error decreases for M smaller than a fixed value $M^\star$ which depends on N ($M^\star = 12$ if $N = 4$, $M^\star = 9$ if $N = 6$); for $M > M^\star$, the problem becomes ill-conditioned and the roots do not converge anymore to the Laplace eigenvalues. This behavior explains also the reason why in Figure 12 only 4 peaks are identified by the LS-Padé approximant. The ill-conditioning of the eigenvalue problem limits the applicability of the method, especially in high frequency regime, where the singularities are dense. To overcome this problem, we are currently investigating the multi-point generalization of the single-point LS-Padé method proposed in this paper. In a multi-point framework, the number of derivatives to be computed are split over the set of centers. In particular, instead of computing $M + N$ derivatives in a single center z_0, $\lceil (M + N)/n \rceil$ derivatives will be computed in each center z_i, for $i = 0, \ldots, n - 1$.
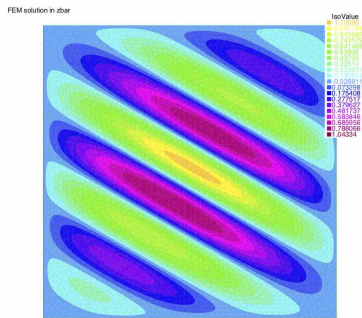

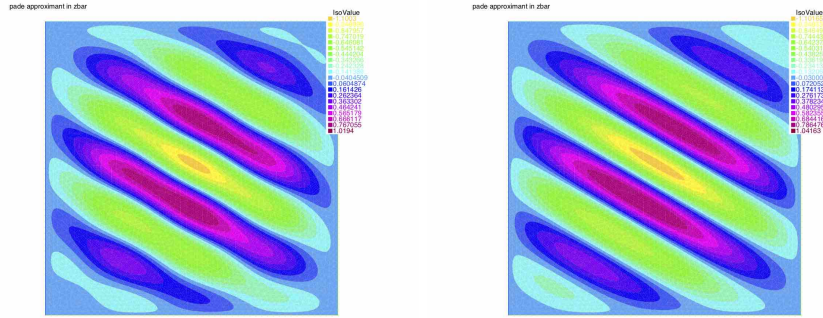Figure 8: Finite element solution $\mathcal{S}_h(51) \in V$ of problem (2)

Figure 9: LS-Padé approximant $\mathcal{S}_{h,P}(51)$ centered in $z_0 = 47+0.5i$, with degrees $M = 10$ and $N = 2$ (left), $N = 4$ (right).
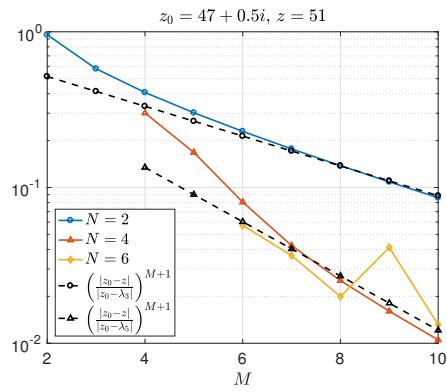

Figure 10: Relative error $\dfrac{\|\mathcal{S}(z)-\mathcal{S}_{h,P}(z)\|_{V,\sqrt{\mathrm{Re}(z_0)}}}{\|\mathcal{S}(z)\|_{V,\sqrt{\mathrm{Re}(z_0)}}}$ in the point $z = 51$, as a function of the degree of the numerator M.
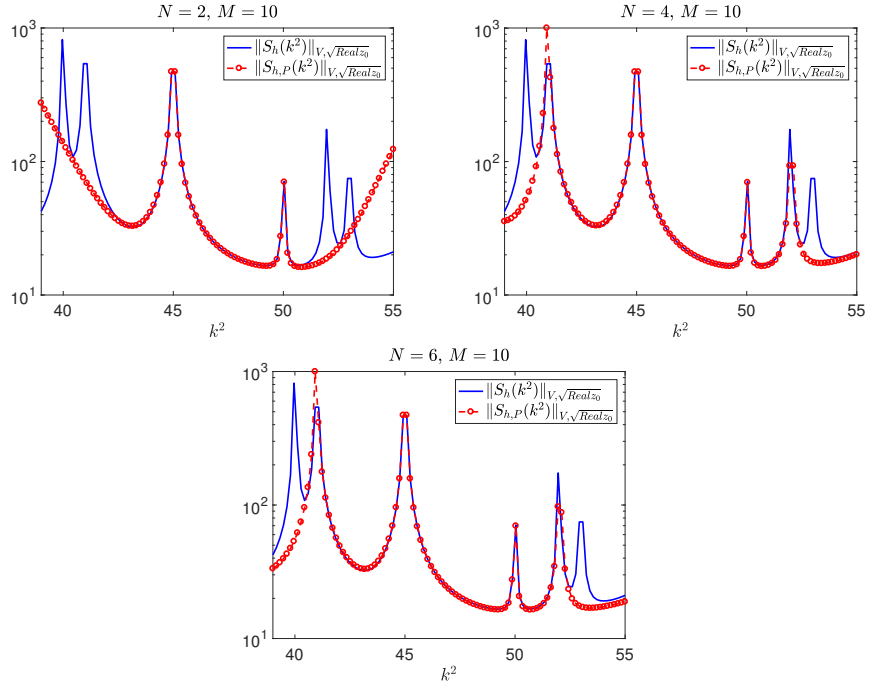
19

Figure 11: Comparison between the weighted $H^1(D)$-norm of the $\mathbb{P}^3$ finite element solution $\mathcal{S}_h(z)$, and the weighted $H^1(D)$-norm of the LS-Padé approximant $\mathcal{S}_{[M/N]}(z)$, for numerator degree $M = 10$ and denominator degree $N = 2$, $N = 4$ and $N = 6$.
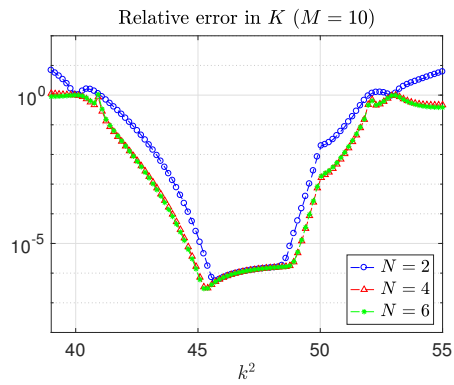

Figure 12: Relative error $\dfrac{\|\mathcal{S}_h(z) - \mathcal{S}_{h,P}(z)\|_{H^1(D),\sqrt{\mathrm{Re}(z_0)}}}{\|\mathcal{S}_h(z)\|_{H^1(D),\sqrt{\mathrm{Re}(z_0)}}}$ for different values of the degree of the denominator.
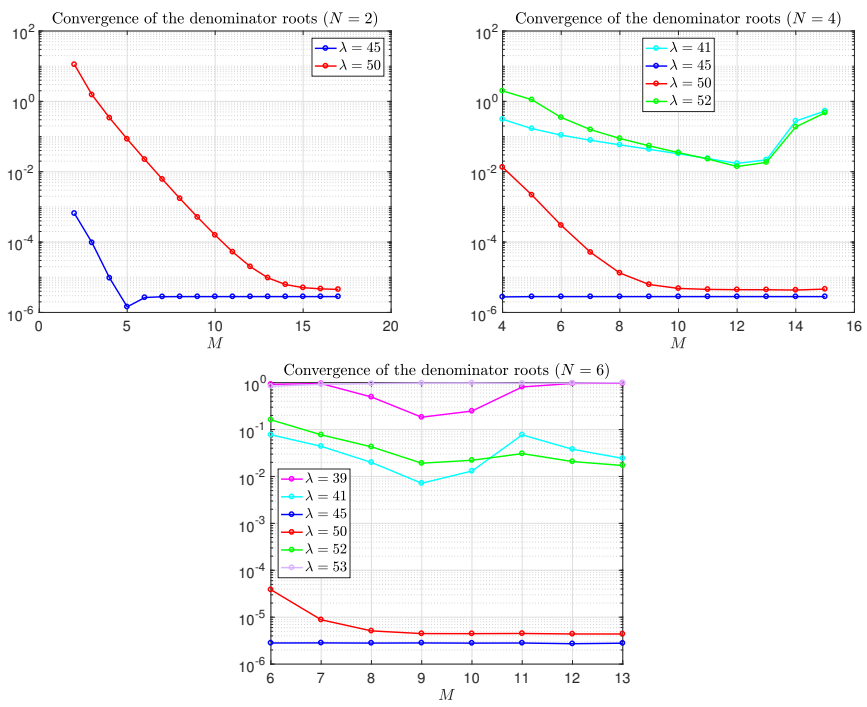
20

Figure 13: Convergence of the roots r_Q of the LS-Padé denominator to the Laplace eigenvalues. The error $|r_Q - \lambda|$ is plotted for $N = 2$, $N = 4$ and $N = 6$.

7 LS-Padé approximant of the stochastic model problem

This section deals with the stochastic counterpart of Problem 1:

Problem 4 (Stochastic Model Problem) *The wavenumber k^2 of the Helmholtz equation is modeled as a random variable with bounded density function $\mathscr{F}_{k^2}$. In this section, either Dirichlet or Neumann or mixed Dirichlet/Neumann homogeneous boundary conditions on ∂D are considered.*

We introduce a Lipschitz functional $\mathcal{L} : V \to \mathbb{R}$ representing a quantity of interest of the frequency response map $\mathcal{S}$, and we define the following two random variables:

$$X := \mathcal{L}(\mathcal{S}(k^2)) \tag{30}$$

and

$$X_P := \mathcal{L}(\mathcal{S}_{[M/N]}(k^2)) \tag{31}$$

where $\mathcal{S}_{[M/N]} = \frac{\mathcal{P}_{[M/N]}}{\mathcal{Q}_{[M/N]}}$ is the LS-Padé approximant of $\mathcal{S}$ centered in z_0, with $\mathrm{Re}\,(z_0) = \frac{k^2_{min}+k^2_{max}}{2}$ and $\mathrm{Im}\,(z_0) \neq 0$; this guarantees that $z_0 \notin \Lambda$, Λ being the set of eigenvalues of the Laplacian, with the considered boundary conditions. Let $\phi_X, \phi_{X_P} : \mathbb{R} \to \mathbb{C}$ denote the characteristic functions of X and X_P, respectively, i.e., $\phi_X(t) := \mathbb{E}\left[e^{itX}\right]$, $\phi_{X_P}(t) := \mathbb{E}\left[e^{itX_P}\right]$. We are interested in studying the LS-Padé approximation error on the characteristic function, i.e., we aim at proving an a priori bound for

$$err_t = |\phi_X(t) - \phi_{X_P}(t)| \quad \text{for any } t \in \mathbb{R}. \tag{32}$$

Theorem 7.1 *Let $\mathcal{L} : V \to \mathbb{R}$ be a Lipschitz functional with Lipschitz constant L, and let X, X_P be the random variables defined in (30) and (31). Given $\alpha > 0$, then it holds*

$$err_t \leq \left(2\,|K_\alpha| + |t|\,L\,C\frac{1}{\alpha^3}\left(\frac{\rho}{R}\right)^{M+1}|K|\right)\sup_{x \in K}\mathscr{F}_{k^2}(x) \quad \forall\, t \in \mathbb{R}, \tag{33}$$

with the same definitions of R, ρ, and K_α, and the same characterization of $C > 0$ as in Theorem 2.4, and $|\cdot|$ denoting the Lebesgue measure.

Proof. Using the definition of the characteristic function and the linearity of the expected value we find

$$err_t = |\phi_X(t) - \phi_{X_P}(t)| = \left|\mathbb{E}\left[e^{itX}\right] - \mathbb{E}\left[e^{itX_P}\right]\right|$$

$$= \left|\mathbb{E}\left[e^{itX} - e^{itX_P}\right]\right| = \left|\int_K \left(e^{it\mathcal{L}(\mathcal{S}(x))} - e^{it\mathcal{L}(\mathcal{S}_{[M/N]}(x))}\right)\mathscr{F}_{k^2}(x)\,dx\right|$$

$$\leq \left|\int_{K_\alpha}\left(e^{it\mathcal{L}(\mathcal{S}(x))} - e^{it\mathcal{L}(\mathcal{S}_{[M/N]}(x))}\right)\mathscr{F}_{k^2}(x)\,dx\right|$$

$$+ \left|\int_{K \setminus K_\alpha}\left(e^{it\mathcal{L}(\mathcal{S}(x))} - e^{it\mathcal{L}(\mathcal{S}_{[M/N]}(x))}\right)\mathscr{F}_{k^2}(x)\,dx\right|.$$

We bound the two integrals separately. For the integral over K_α, we have

$$\left|\int_{K_\alpha}\left(e^{it\mathcal{L}(\mathcal{S}(x))} - e^{it\mathcal{L}(\mathcal{S}_{[M/N]}(x))}\right)\mathscr{F}_{k^2}(x)\,dx\right|$$

$$\leq \int_{K_\alpha}\left|e^{it\mathcal{L}(\mathcal{S}(x))}\right|\mathscr{F}_{k^2}(x)dx + \int_{K_\alpha}\left|e^{it\mathcal{L}(\mathcal{S}_{[M/N]}(x))}\right|\mathscr{F}_{k^2}(x)dx \leq 2\,|K_\alpha|\sup_{x \in K_\alpha}\mathscr{F}_{k^2}(x). \tag{34}$$

Consider now the integral over $K \setminus K_\alpha$. Since e^{itx} is Lipschitz as a function of x with constant $|t|$, and $\mathcal{L}$ is Lipschitz with constant L, we find

$$\left| \int_{K \setminus K_\alpha} \left(e^{it\mathcal{L}(\mathcal{S}(x))} - e^{it\mathcal{L}(\mathcal{S}_{[M/N]}(x))} \right) \mathscr{F}_{k^2}(x)\, dx \right|$$

$$\leq \int_{K \setminus K_\alpha} \left| e^{it\mathcal{L}(\mathcal{S}(x))} - e^{it\mathcal{L}(\mathcal{S}_{[M/N]}(x))} \right| \mathscr{F}_{k^2}(x) dx$$

$$\leq |t| \int_{K \setminus K_\alpha} \left| \mathcal{L}(\mathcal{S}(x)) - \mathcal{L}(\mathcal{S}(x))_{[M/N]} \right| \mathscr{F}_{k^2}(x) dx$$

$$\leq |t|\, L \int_{K \setminus K_\alpha} \left\| \mathcal{S}(x) - \mathcal{S}(x)_{[M/N]} \right\|_{V, \sqrt{\mathrm{Re}(z_0)}} \mathscr{F}_{k^2}(x) dx.$$

From the bound (7) of Theorem 2.4, we obtain

$$\left| \int_{K \setminus K_\alpha} \left(e^{it\mathcal{L}(\mathcal{S}(x))} - e^{it\mathcal{L}(\mathcal{S}_{[M/N]}(x))} \right) \mathscr{F}_{k^2}(x)\, dx \right|$$

$$\leq |t|\, L\, C \frac{1}{\alpha^3} \left(\frac{\rho}{R} \right)^{M+1} |K| \sup_{x \in K \setminus K_\alpha} \mathscr{F}_{k^2}(x). \tag{35}$$

The conclusion follows from inequalities (34) and (35). $\qquad\square$

Corollary 7.2 *Under the same assumptions as in Theorem 7.1, it holds*

$$\lim_{M \to \infty} err_t = 0 \quad \forall t \in \mathbb{R}.$$

In particular, there exists $C > 0$ such that for any $t \in \mathbb{R}$

$$err_t \leq C\, |t|^{1/4} \left(\frac{\rho}{R} \right)^{\frac{M+1}{4}}.$$

Proof. We have $|K_\alpha| \leq \alpha n$, with $n \leq N$ the number of poles of $\mathcal{S}$ in K. From Theorem 7.1 it holds
$$err_t \leq \inf_{\alpha > 0} \left(C_1 \alpha + C_2(t) \frac{1}{\alpha^3} \left(\frac{\rho}{R} \right)^{M+1} \right),$$
with $C_1 = 2n \sup_{x \in K} \mathscr{F}_{k^2}(x)$ and $C_2(t) = |t|\, LC\, |K|\, \mathscr{F}_{k^2}(x)$. By optimizing the expression in α we obtain
$$err_t \leq C_t \left(\frac{\rho}{R} \right)^{\frac{M+1}{4}}$$
with $C_t = C_1^{3/4} C_2(t)^{1/4} (3^{1/4} + 3^{-3/4})$. $\qquad\square$

This corollary establishes, in particular, uniform exponential convergence of ϕ_{X_P} to ϕ_X on any compact subset of $\mathbb{R}$.

Remark 7.3 *Theorem 7.1 and Corollary 7.2 can be generalized to derive an a priori upper bound on $err_\xi = |\mathbb{E}[\xi(X)] - \mathbb{E}[\xi(X_P)]|$, for any continuous and bounded functional $\xi : \mathbb{R} \to \mathbb{R}$. Thus, the weak convergence of X_P to X follows, as $M \to +\infty$.*

Let us consider the case of $\partial D = \Gamma_D$. Let $K = [7, 14]$ be the interval of interest (which contains three eigenvalues of the Dirichlet-Laplace operator: $8, 10, 13$), and let the wavenumber be modeled as a random variable uniformly distributed on K, i.e., $k^2 \sim \mathcal{U}(K)$. Given the functional $\mathcal{L} = \|\cdot\|_{V, \sqrt{\mathrm{Re}(z_0)}}$, where $z_0 = 10 + 0.5i$, we consider the random variables $X = \left\| \mathcal{S}_h(k^2) \right\|_{V, \sqrt{\mathrm{Re}(z_0)}}$ and $X_P = \left\| \mathcal{S}_{h,P}(k^2) \right\|_{V, \sqrt{\mathrm{Re}(z_0)}}$. We define as

$\mathcal{S}_h$ the $\mathbb{P}^3$ finite element approximation of $\mathcal{S}$; then $\mathcal{S}_{h,P}$ is the LS-Padé approximant of $\mathcal{S}_h$, centered in z_0 and with polynomial degrees (M, N). In Figure 14, we display the random variables X and X_P evaluated at 100 sample points uniformly distributed in K. When the degree of the LS-Padé denominator is $N = 3$, all the poles are correctly identified by the LS-Padé approximant, provided that M is larger than 4. In Figure 15 we plot the characteristic function of the random variable X_P, $\phi_{X_P}(t)$, where the degrees of the Padé denominator and denominator are $N = 3$, and $M = 2, 4, 6$, respectively. The expected value has been computed by the Monte Carlo method, using 10^5 samples.
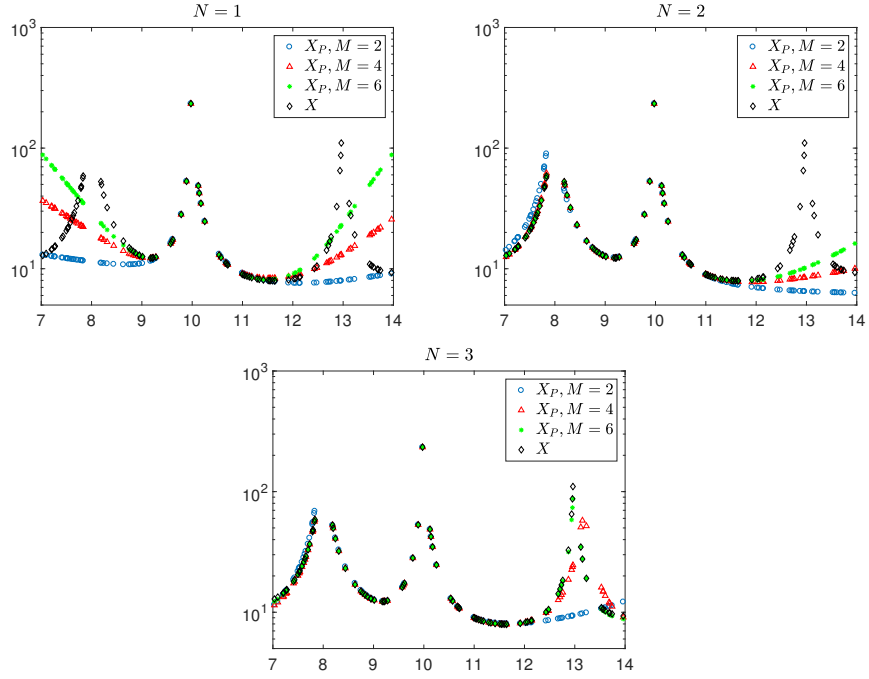

Figure 14: Comparison between $X = \left\|\mathcal{S}_h(k^2)\right\|_{V, \sqrt{\mathrm{Re}(z_0)}}$ and $X_P = \left\|\mathcal{S}_{h,P}(k^2)\right\|_{V, \sqrt{\mathrm{Re}(z_0)}}$ evaluated at 100 sample points uniformly distributed in $K = [7, 14]$).
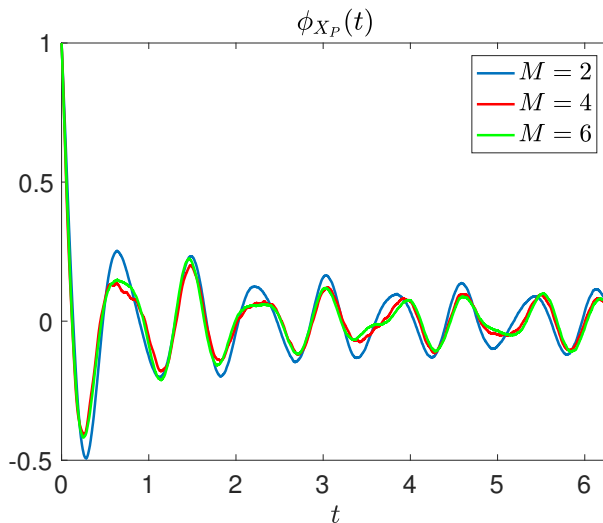
Figure 15: Characteristic function $\phi_{X_P}(t)$, with $N = 3$ and $M = 2, 4, 6$.

8 Conclusions

The present paper concerns a model order reduction method based on the single-point LS-Padé approximation technique introduced in [3]. We have described an algorithm to compute the LS-Padé approximant of the Helmholtz frequency response map, and we have explored the applicability and potentiality of the method via 2D numerical experiments in various contexts. Moreover, the time-harmonic wave equation with random wavenumber has been analyzed.

We are currently investigating the extension of the proposed methodology and of its convergence analysis to the case of *multi-point* LS-Padé expansions, where evaluations of the frequency response map $\mathcal{S}$ and of its derivatives at multiple frequencies are used. We believe that this technique will outperform the single-point one, when a large number of singularities of $\mathcal{S}$ need to be identified.

References

[1] R. A Adams and J. JF Fournier. *Sobolev Spaces*, volume 140. Academic press, 2003.

[2] I. M. Babuška and S. A. Sauter. Is the pollution effect of the FEM avoidable for the Helmholtz equation considering high wave numbers? *SIAM Journal on Numerical Analysis*, 34(6):2392–2423, 1997.

[3] F. Bonizzoni, F. Nobile, and I. Perugia. Convergence analysis of Padé approximations for Helmholtz frequency response problems. *ESAIM: M2AN.*, 2017. Online (DOI: 10.1051/m2an/2017050).

[4] F. Bonizzoni, F. Nobile, I. Perugia, and D. Pradovera. Fast Least-Squares Padé approximation of self-adjoint problems with meromorphic structure. In preparation.

[5] Y. Chen, J.S. Hesthaven, Y. Maday, and J. Rodríguez. Certified reduced basis methods and output bounds for the harmonic Maxwell's equations. *SIAM J. Sci. Comput.*, 32(2):970–996, 2010.

[6] O. Ezvan, A. Batou, C. Soize, and L. Gagliardini. Multilevel model reduction for uncertainty quantification in computational structural dynamics. *Computational Mechanics*, 59(2):219–246, 2017.

[7] P. Guillaume, A. Huard, and V. Robin. Generalized multivariate Padé approximants. *Journal of Approximation Theory*, 95(2):203 – 214, 1998.

[8] S. Hain, M. Ohlberger, M. Radic, and K. Urban. A Hierarchical A-Posteriori Error Estimatorfor the Reduced Basis Method. *ArXiv e-prints*, 2018.

[9] U. Hetmaniuk, R. Tezaur, and C. Farhat. Review and assessment of interpolatory model order reduction methods for frequency response structural dynamics and acoustics problems. *International Journal for Numerical Methods in Engineering*, 90(13):1636–1662, 2012.

[10] U. Hetmaniuk, R. Tezaur, and C. Farhat. An adaptive scheme for a class of interpolatory model reduction methods for frequency response problems. *International Journal for Numerical Methods in Engineering*, 93(10):1109–1124, 2013.

[11] R. Hiptmair, A. Moiola, and I. Perugia. Trefftz discontinuous Galerkin methods for acoustic scattering on locally refined meshes. *Applied Numerical Mathematics*, 79:79–91, 2014.

[12] R. Hiptmair, L. Scarabosio, C. Schillings, and C. Schwab. Large deformation shape uncertainty quantification in acoustic scattering. *Advancces in Computational Mathematics*, 2018.

[13] A. Huard and V. Robin. Continuity of approximation by least-squares multivariate Padé approximants. *Journal of Computational and Applied Mathematics*, 115(1–2):255 – 268, 2000.

[14] D. B. P. Huynh, G. Rozza, S. Sen, and A.T. Patera. A successive constraint linear optimization method for lower bounds of parametric coercivity and inf-sup stability constants. *Comptes Rendus Mathematique*, 345(8):473 – 478, 2007.

[15] D. B. P. Huynh, D. B. P. A static condensation reduced basis element approximation: Application to three-dimensional acoustic muffler analysis. *International Journal of Computational Methods*, 11(03):1343010, 2014.

[16] E. Jacquelin, O. Dessombz, J.-J. Sinou, S. Adhikari, and M. I. Friswell. Polynomial chaos-based extended Padé expansion in structural dynamics. *International Journal for Numerical Methods in Engineering*, 111(12):1170–1191, 2017.

[17] E. Jacquelin, O. Dessombz, J.-J Sinou, S. Adhikari, and M.I. Friswell. Steady-state response of a random dynamical system described with Padápproximants and random eigenmodes. *Procedia Engineering*, 199:1104 – 1109, 2017. X International Conference on Structural Dynamics, EURODYN 2017.

[18] S. Kapita, P. Monk, and T. Warburton. Residual-based adaptivity and PWDG methods for the Helmholtz equation. *SIAM Journal on Scientific Computing*, 37(3):A1525–A1553, 2015.

[19] T. Lassila, A. Manzoni, and G. Rozza. On the approximation of stability factors for general parametrized partial differential equations with a two-level affine decomposition. *ESAIM: Mathematical Modelling and Numerical Analysis*, 46(6):1555–1576, 2012.

[20] M. Lenoir, M. Vullierme-Ledard, and C. Hazard. Variational formulations for the determination of resonant states in scattering problems. *SIAM Journal on Mathematical Analysis*, 23(3):579–608, 1992.

[21] W. C. H. McLean. *Strongly elliptic systems and boundary integral equations*. Cambridge university press, 2000.

[22] D. Modesto, S. Zlotnik, and A. Huerta. Proper generalized decomposition for parameterized Helmholtz problems in heterogeneous and unbounded domains: Application to harbor agitation. *Computer Methods in Applied Mechanics and Engineering*, 295:127 – 149, 2015.

[23] R. Ohayon and C. Soize. Computational Vibroacoustics in Low- and Medium-Frequency Bands: Damping, ROM, and UQ Modeling. *Applied Sciences-Basel*, 7(6), 2017.

[24] C. Schwab and C. J. Gittelson. Sparse tensor discretizations of high-dimensional parametric and stochastic PDEs. *Acta Numerica*, 20:291–467, 2011.

[25] S. Sen. *Reduced basis approximation and a posteriori error estimation for noncoercive elliptic problems: applications to acoustics*. PhD thesis, Massachusetts Institute of Technology, 2007.

[26] S. Sen, K. Veroy, D. B. P. Huynh, S. Deparis, N. C. Nguyen, and A. T. Patera. "Natural norm" a posteriori error estimators for reduced basis approximations. *J. Comput. Phys.*, 217(1):37–62, 2006.

[27] S. Steinberg. Meromorphic families of compact operators. *Archive for Rational Mechanics and Analysis*, 31(5):372–379, Dec 1968.

[28] T. Tonn, K. Urban, and S. Volkwein. Comparison of the reduced-basis and POD a posteriori error estimators for an elliptic linear-quadratic optimal control problem. *Mathematical and Computer Modelling of Dynamical Systems*, 17(4):355–369, 2011.

[29] K. Veroy, C. Prud'Homme, D.V. Rovas, and A.T. Patera. A posteriori error bounds for reduced-basis approximation of parametrized noncoercive and nonlinear elliptic partial differential equations. 2003.